IEEE Access
Multidisciplinary | Rapid Review | Open Access Journal

Received November 21, 2017, accepted December 16, 2017, date of publication January 3, 2018,
date of current version February 28, 2018.

Digital Object Identifier 10.1109/ACCESS.2017.2788179

Wideband RF Self-Interference Cancellation Circuit for Phased Array Simultaneous Transmit and Receive Systems

SATHEESH BOJJA VENKATAKRISHNAN, (Member, IEEE), ELIAS A. ALWAN, (Member, IEEE), AND JOHN L. VOLAKIS, (Fellow, IEEE)

Department of Electrical and Computer Engineering, Florida International University, Miami, FL 33174, USA

Corresponding author: Satheesh Bojja Venkatakrishnan (sbojjave@fiu.edu)

This work was supported by the Office of Naval Research, Arlington, VA, USA, under Grant N00014-16-1-2253.

ABSTRACT With the growing demand for spectrum utilization, the concept of full duplex transceivers has become attractive. These simultaneous transmit and receive systems (STAR) are attractive as they double bandwidth utilization. To realize STAR, we must suppress self-interference (SI) between transmit and receive antennas. Doing this across a wide bandwidth presents an even greater challenge. Further, for antenna arrays, SI can be higher due to mutual coupling among neighboring elements. In this paper, we achieve 100 dB isolation for practical STAR, across a large 500 MHz bandwidth. Specifically, four stages of the self-interference cancellation are proposed. In addition to high isolation cross-polarized array elements, we employ multi-tap filters at the transceiver RF front-end for interference cancellation. These filters emulate direct SI coupling using frequency-domain optimization techniques. Measured results show an average of 25 dB filter cancellation is possible across 500 MHz.

INDEX TERMS RF Cancellation, self-interference cancellation, wideband interference cancellation, in-band full duplex, simultaneous transmit and receive.

I. INTRODUCTION

With the current congested spectrum, it is difficult to find continuous frequency bands for ultra wideband (UWB) transmission [1]–[3]. This need for contiguous spectrum has led to creative approaches of spectrum allocation and re-use [1], [2], [4]–[7], including in-band full duplex systems. Current systems either employ frequency division duplexing (FDD) or time division duplexing (TDD) to realize full duplex. These realizations, rely on the orthogonality of time/frequency resources to avoid interference between the transmit and receive signals. However, both FDD and TDD require double the time and/or frequency resources as compared to full duplex systems. Further, multiband communication systems that employ the FDD technique require a large number of tunable duplexers, implying a complex RF architecture and large form factors. Such systems are generally lossy as well. Notably, TDD communication systems do not require a duplexer. Rather, they require isolators to suppress interference between the uplink and downlink channels [8], [9].

Simultaneous transmit and receive (STAR) systems, also referred to as in-band full-duplex (IBFD) or division free duplexing (DFD), have the potential to overcome these shortcomings [1], [2], [4]–[7]. In STAR, spectral efficiency is theoretically doubled, when transmission and reception happen at the same time and at the same frequency [1]. Furthermore, from a wireless network perspective, frequency planning is simpler, since only a single frequency need be shared between uplink and downlink. Another possible advantage is that they can also sense network traffic to provide enhanced interference coordination. Despite the various benefits offered by STAR, there are several issues preventing their practical implementation. The main issue though stems from coupling of the transmit signals due to their proximity to the receiver, causing receiver desensitization [1], [2], [4]–[7], [10].

To improve spectral efficiency using STAR, we must suppress self-interference (SI) due to coupling between the transmitter and receiver. Typically, SI includes direct and reflected/echo/multipath signals, harmonics from the power amplifier (PA), and noise from the transmit chain. Thus, any self-interference cancellation (SIC) architecture should be able to model and predict these distortions to achieve full duplex operation [6], [11]. To prevent receiver saturation, the interfering signal must be sufficiently canceled at the

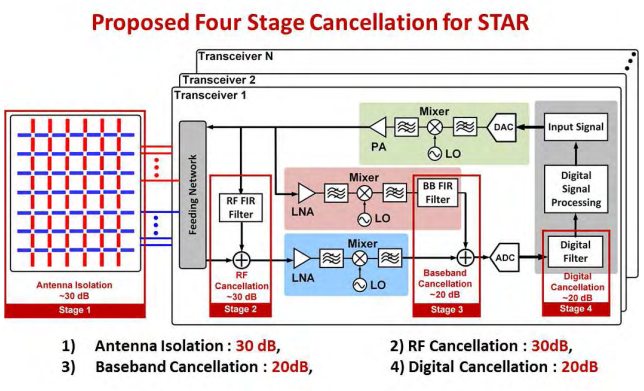

FIGURE 1. STAR system showing multi-stage 100 dB cancellation across a wide bandwidth for a system with *N* transceivers and antenna elements.

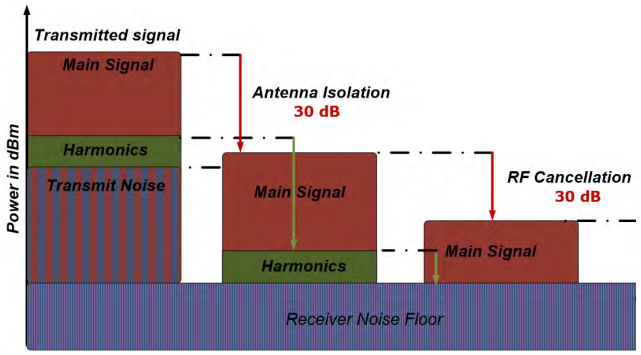

FIGURE 2. Self-interference cancellation across the first two stages of the proposed STAR system.

RF stages. In addition, digital cancellation algorithms must be employed to remove nonlinear distortions at the backend.

Recent STAR implementations include cancellation stages at the antenna, RF, and digital domains. Such multi-stage cancellation are necessary to achieve up to 100 dB cancellation across the operational bandwidth. In [6], a 16-tap filter with fixed delays and programmable attenuators were presented to achieve high cancellation of 47 dB. However, this was across a narrow bandwidth of 80 MHz. Time domain equalization approaches using sampling and interpolation techniques were employed to achieve this. Another approach using frequency domain equalization was reported in [4]. In this approach, multiple RF bandpass filters (BPF) were included in the canceler. The latter was used to channelize the desired bandwidth (BW). Using this approach, RF self-interference cancellation (RF-SIC) of 20 dB across 27 MHz was achieved. In [2], a 4-tap filter with variable delays and attenuators was used using time-domain transmission techniques for high transmit power applications. Under this condition, an SIC of 30 dB was achieved across a 30 MHz bandwidth.

In this paper, a new STAR architecture is proposed to achieve much greater measure of self-interference cancellation (SIC) across a large bandwidth of 500 MHz. As can be expected, larger bandwidths imply more stringent requirements on SIC. To achieve SIC across a 500 MHz bandwidth, we propose four cancellation stages [12]–[14], as depicted in Fig. 1. These stages include: a) 30 dB antenna isolation [15], [16], b) 30 dB radio frequency (RF) analog cancellation [7], [11], [17]–[19], c) baseband (BB) analog cancellation of 20 dB [20], and d) digital cancellation of 20 dB [11], [21].

This paper focuses on the RF-SIC (Stage-2) circuit to provide cancellation across a 500 MHz bandwidth. Concurrently, to achieve high antenna isolation, we employed an UWB antenna array with collocated cross dipole elements, depicted in Fig. 1. Port-to-port coupling isolation ranging from 20 dB to 35 dB across 2.6 GHz to 4 GHz was achieved. The RF-SIC filter serves to achieve an additional 30 dB of cancellation after the antenna. To do so, a 6-tap finite impulse response (FIR) filter is designed and fabricated. The FIR filter mimics the response of the antenna coupling across 500 MHz. Experimental results show that for the designed RF-SIC filter (stage-2), 17 dB to 33 dB cancellation across a 500 MHz bandwidth can be achieved. These results demonstrate that tunable multi-tap filters are the most promising and cost effective methods of achieving significant cancellation across a wide bandwidth. To our knowledge, this is the first RF-SIC filter that can achieve such wide bandwidth.

This paper is structured as follows. Section II describes the first two cancellation stages employed in this STAR architecture. Mathematical representations of the cancellation process and implementation details are described. The stage-2 RF cancellation filter design and fabrication are described in Section III. Measurements are given in Section IV.

II. STAR CANCELLATION STAGES

As depicted in Fig. 1, the first cancellation stage (Stage-1) involves the suppression of the coupled signal at the antenna stage. It is crucial to achieve good isolation at the antenna stage as suppression at this stage relaxes SIC requirements at subsequent stages. Prior work using multi-antenna STAR systems employed path loss, cross-polarization, and beamforming techniques to achieve 47 dB cancellation in multipath environments. However, this was done across a very narrow bandwidth [6], [11], [18], [21], [22].

RF cancellation (Stage-2 in Fig. 1) involves tapping a replica of the transmitted signal prior to transmission. This signal is then adjusted using RF filter circuits and combined with the received signal for cancellation [23]. The first two stages, namely antenna isolation and RF cancellation, are important as they suppress transmitter non-idealities and transmit chain noise below the receiver noise floor. Doing so, prevents low noise amplifier (LNA) and analog-to-digital converter (ADC) saturation. Hence, it is crucial that the first two stages, achieve a combined 60 dB cancellation, as shown in Fig. 2. Unlike recent STAR implementations that were of narrow bandwidth (<100 MHz), in this paper we pursue cancellation across a large 500 MHz bandwidth.

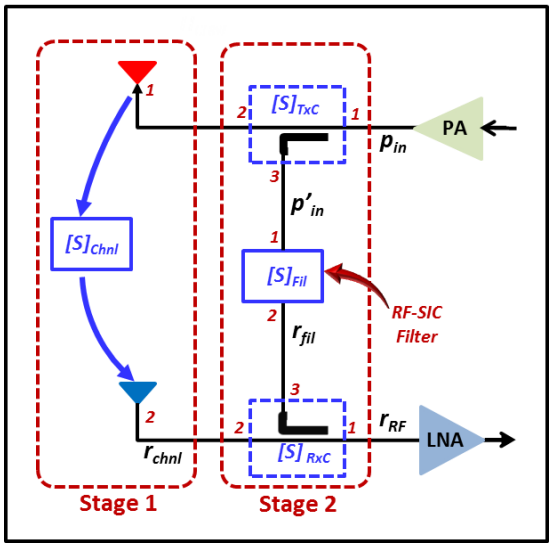

FIGURE 3. Block diagram showing the proposed STAR cancellation approach performed in the RF domain using the coupled signal from the antenna and the filtered signal from RF-SIC.

Additional stages of cancellation include analog baseband and digital cancellations. In the analog baseband stage, a copy of transmitted signal is downconverted to baseband and used to suppress the coupled signal. As a result, the coupled baseband signals are suppressed by 20 dB. A fourth stage of cancellation can also be implemented in the digital backend to achieve an additional 20 dB of cancellation. To do so, the transmit bits are stored in memory, then used to cancel out the residual coupled signal. The additional 2 stages are required to achieve a total 100 dB of SIC. However, these stages are outside the scope of this paper. They are depicted in Fig. 1 for completeness. In the following sections, the implementation of the RF-SIC filter is described

A. RF CANCELLATION STAGE

To achieve 30 dB SIC across a 500 MHz bandwidth, we will employ a multi-tap FIR filter. Already, various single-tap filters have demonstrated SIC reduction of the transmit-receive coupling. However, these designs have been across narrow instantaneous bandwidths [10], [21], [24]. The proposed multi-tap FIR filter designs provide more degrees of freedom (such as tunable tap delay and attenuation at each taps) to achieve much larger bandwidth. As shown in Fig. 1, this cancellation signal is sourced from the transmit chain immediately after the power amplifier (PA), thereby including nonlinearities. It is then injected into the primary receiver path before passing through the LNA of the receiver.

The main goal of the RF stage is to suppress the RF transmit signal that couples into the receiver side. A simple block diagram depicting the first two stages of STAR is given in Fig. 3. As can be seen, a directional coupler is employed at the input and output ports of the transceiver. That is, a small portion of the transmitted signal p_{in} from the PA is coupled to stage-2. The rest of the signal is sent to the

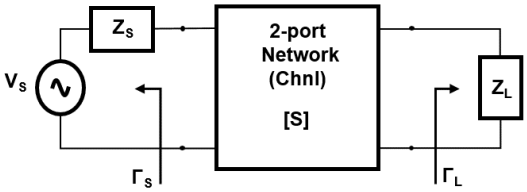

FIGURE 4. Two-port block diagram describing the signal flow across the transmit/receive ports.

antenna for transmission. At the receiver side, a directional coupler is employed to combine the signals from the receiving antenna and the stage-2 RF-FIR filter. To achieve maximum cancellation, the signal r_{RF} (see Fig. 3) must be ideally zero. This occurs when the following condition holds

$$S21_{TxC}S21_{chnl}S12_{RxC} = -(S31_{TxC}S21_{fil}S13_{RxC}). \quad (1)$$

In other words,

$$\begin{aligned} &|S21_{TxC}||S21_{chnl}||S12_{RxC}| \\ &\quad = |S31_{TxC}||S21_{fil}||S13_{RxC}| \\ &\angle S21_{TxC} + \angle S21_{chnl} + \angle S12_{RxC} \\ &\quad = \angle S31_{TxC} + \angle S21_{fil} + \angle S13_{RxC} + 180^\circ. \end{aligned} \quad (2)$$

In the above, *Sij* corresponds to the scattering parameters ([S] matrix) at each junction. Also, the subscripts *TxC*, *chnl*, *fil* and *RxC* correspond to the junction or coupling ports. Specifically, *TxC* = transmit chain, *chnl* = antenna coupling response (or channel), *fil* = RF-SIC filter, and *RxC* = receive chain. In (2),to achieve signal cancellation the phases of the coupled and filtered signals must be 180° out of phase.

The characteristics of the transmit to receive antenna junction is referred to as '*chnl*', and can be measured in the anechoic chamber. Ignoring multipath signals, the coupled signal is influenced by its closest N-transmit antenna elements. This coupling must be accounted for. Referring to Fig. 4, the transfer function ($H_{chnl}(j\omega)$) represents the coupling from the trasnmitting antenna to the receiving port #2, as given by [25]

$$\begin{aligned} &H_{chnl}(j\omega) \\ &= S21_{chnl}\Big[(1-\Gamma_L)(1-\Gamma_S) \\ &\quad \times \frac{1}{(1-S22_{chnl}\Gamma_L)(1-S11_{chnl}\Gamma_S) - S12_{chnl}S21_{chnl}\Gamma_L\Gamma_S}\Big]. \end{aligned} \quad (3)$$

In the above, Γ_S and Γ_L are the source and load reflection coefficients, respectively. Further, the antenna elements are designed to be matched to 50Ω loads across the entire operational bandwidth. Hence, they have low return loss of < -15 dB as depicted in the voltage standing wave ratio (VSWR) plots in [26]. Under this assumption, $S11_{chnl} = S22_{chnl} = \Gamma_L = \Gamma_S \approx 0$. Simplifying (3) to

$$H_{chnl}(j\omega) = S21_{chnl}. \quad (4)$$

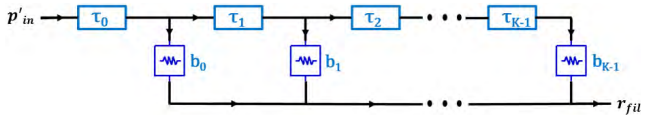

FIGURE 5. RF-SIC FIR filter topology using delay lines and tap coefficients as attenuators.

Henceforth, $S21_{chnl}$ and $H_{chnl}(j\omega)$ will be used interchangeably.

We want to consider the coupling between specific elements n and i. In this particular case, the impulse response is described as $h_{chnl,n,i}(t)$, where i refers to the coupling of the i^{th} transmit antenna to the n^{th} receive antenna. When considering all N transmitting elements from $i = 1$ to $i = N$, we have

$$H_{chnl,n}(j\omega) = \sum_{i=1}^{N} H_{chnl,n,i}(j\omega) = \sum_{i=1}^{N} S_{n,i}. \quad (5)$$

The goal is to design a filter whose response cancels the coupling $H_{chnl,n}(j\omega)$. The transfer function of the RF filter can be represented using filter taps as,

$$H_{fil,n}(j\omega) = \sum_{k=0}^{K-1} b_k e^{-j\omega\tau_k} \quad (6)$$

where b_k are the tap coefficient value and τ_k are the delay taps. Our goal is to find b_k and τ_k such that the condition given in (2) is valid. The following section describes the procedure to extract b_k and τ_k. Subsequently, using the b_k and τ_k values, the RF-FIR can be realized.

To achieve maximum SIC, our goal is to design a filter that replicates precisely the response of the antenna coupling given by (5). To do so, we refer to Fig. 5. The circuit shown is a set of weights and delay line segments. Thus, our next step is to realize the RF filter response $H_{fil,n}(j\omega)$ using the circuit in Fig. 5.

III. SELF-INTERFERENCE CANCELLATION (RF-SIC) RF FILTER DESIGN

To realize the RF-SIC filter we considered equal power splitter and power combiners. That is, we employed an ideal 3-dB direction coupler at the transmit and the receive chain. Referring to Fig. 3, this implies that

$$|S21_{TxC}| = |S12_{RxC}| = |S31_{TxC}| = |S13_{RxC}| = \frac{1}{\sqrt{2}}. \quad (7)$$

Further, we assumed that no phase imbalance exist in the transmit and receive 3-dB direction couplers. Hence, the expression in (2) reduces to,

$$\begin{aligned} |S21_{chnl}| &= |S21_{fil}| \\ \angle S21_{chnl} &= \angle S21_{fil} + 180^\circ. \end{aligned} \quad (8)$$

To design the RF-SIC filter using a multi-tap approach, the coefficient of the transfer function in (6) is optimized to match the coupled signal from the transmitter to the receiver. This optimization must account for the cancellation bandwidth, circuit complexity, as well as acceptable errors and deviations from the target response. Further, on employing a multi-tap FIR filter with tunable parameters (b_k and τ_k) we retain an extra degree of freedom required to achieve large bandwidth operation. To do so, we will use the data representing the measured antenna response $H_{chnl,n}(j\omega)$.

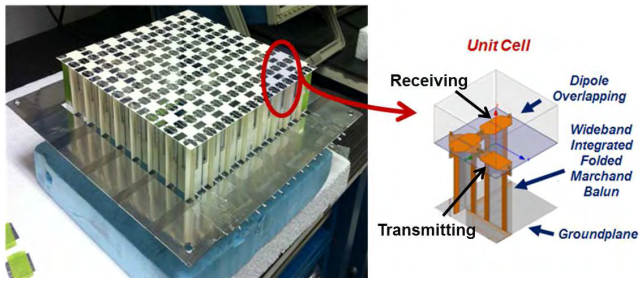

FIGURE 6. 8×8 cross-dipole antenna array with its unit cell representation [26].

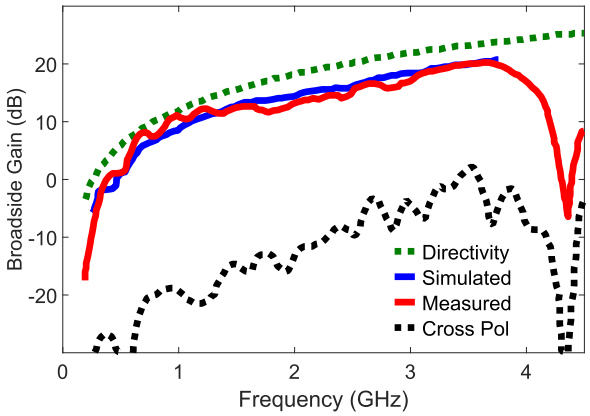

FIGURE 7. Measured and simulated broadside gain of the 8×8 cross-dipole antenna array [26].

In order to measure the antenna response ($H_{chnl,n}(j\omega)$), we employ an UWB 8 × 8 antenna array with collocated crossed dipole elements operating across a 13.1:1 bandwidth and providing 20 dB to 35 dB isolation from 2.6 GHz to 4 GHz. This isolation is based upon exploiting a) polarization orthogonality between transmit and receive antennas, b) symmetric and balanced feeding, and c) suppression of common modes that may exist within the feeding network [16]. The array's unit cell is shown in Fig. 6, and consists of crossed overlapping dipoles, one transmitting and the other receiving, each fed by an integrated Marchand balun. The operational details of this antenna array are reported in [26]. The broadside antenna array gain and cross-coupling characteristics are given in Fig. 7.

In a tightly coupled array configuration, mutual coupling among nearby elements influences performance quite drastically [27], [28]. This mutual coupling must therefore be considered in achieving high isolation between the transmitter and receiver ports. Referring to Fig. 8, the coupling

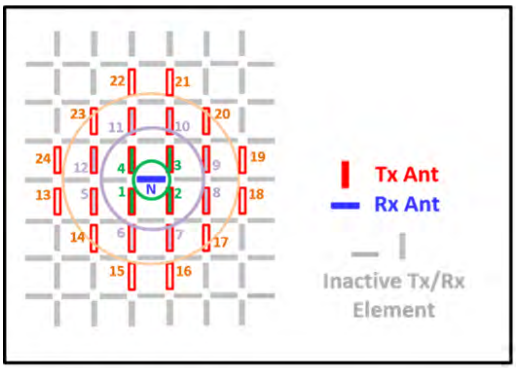

FIGURE 8. Pictorial representation of cross-coupling from neighboring antenna array elements on the center receive element.

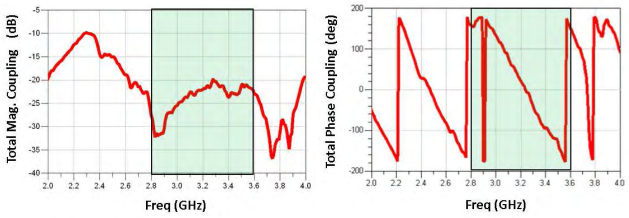

(a) (b)

FIGURE 9. Anechoic chamber port-to-port coupling measurements of the antenna array in Fig. 6, with single element receiving while all surrounding elements are active (a) Magnitude $|S_n(j\omega)|$ and (b) Inverted Phase response $S_n(j\omega)$ of the port-to-port coupling when all surrounding antenna elements transmit and only a single center element is receiving.

from nearby array elements is measured by exciting 24 transmit elements around a single receive element. As expected, the transmit elements, closest to the receiving dipole give the majority of cross-coupling. Therefore, coupling beyond the 24 surrounding elements was not included as it was found negligible. For our case, we will design a filter of order K using a polynomial fit to match the antenna ($chnl$) magnitude and phase response, shown in Fig. 9. This is the measured coupling into the n^{th} port when entire antenna array is transmitting.

Our goal is to find b_k and τ_k such that, $H_{fil,n}(j\omega) \approx H_{chnl,n}(j\omega)$. Based on this filter response, we can then compute the error between the desired and achieved response. Specifically, we have

$$\begin{aligned} |H_{fil,n}(j\omega)| &= |H_{chnl,n}(j\omega)| \pm \Delta_{mag}(j\omega) \\ \angle H_{fil,n}(j\omega) &= \angle H_{chnl,n}(j\omega) + 180^\circ \pm \Delta_{phase}(j\omega) \end{aligned} \quad (9)$$

where, Δ_{mag} and Δ_{phase} refer to the magnitude and phase errors, respectively. Many factors contribute to the error, including power divider mismatch, unaccounted nonidealities in transmit chain, as well as errors related to the antenna response characterization. Based on the data sheets of the components employed, the total error due to the above mentioned nonidealities account for-no more than 3%.

(a) (b)

FIGURE 10. Fabricated RF-SIC filter. (a) Photo of the fabricated 6th order RF-SIC filter, (b) S-parameter measurement setup.

The overall error is then given by

$$Error_{fil,n} = \sqrt{\frac{\int_{\omega_{low}}^{\omega_{high}} \left[\Delta_{mag}{}^2(j\omega) + \Delta_{phase}{}^2(j\omega)\right] d\omega}{\omega_{high} - \omega_{low}}}. \quad (10)$$

Based on the above equation, to emulate the coupling for the antenna, we found that a filter of order $K = 6$ gives a magnitude and phase error on the order of 3% . This error was computed using (10). Notably, for $K = 10$, this error reduces to 0.7% . However, realizing a 10-tap filter is very challenging both in terms of design and integration. Increasing the filter taps results in increasing the number of variables that needs to be optimized. The latter exacerbates the computation complexity. Further, as the number of taps increases, the RF-FIR filter foot print also increases. As a result, the filter integration with antenna array feeding network becomes more challenging.

Below, we fabricate and test the $K = 6$ filter for validation purposes. The b_k and τ_k filter coefficients were obtained using the Gradient Decent algorithm. The specific filter taps are $b_k = \{2.02, 1.27, 2.16, 9.9, 1.258, 2.66\}$ and $\tau_k = \{33, 166, 241, 23, 26, 147\}ps$ at the center frequency. In practice, however, we will use attenuators to represent b_k and microstrip delay lines generated using the linecalc tool in ADS to represent τ_k. ADS Momentum was also used to conduct full-wave simulations of the resulting RF filter. Initial simulations were carried out using a TMM10 substrate having $\epsilon_r = 9.8$ and $tan\delta = 0.0022$. This substrate was chosen due to its higher $\epsilon_r = 9.8$, implying smaller footprint for integration within the antenna array.

The RF-FIR filter was matched to a 50Ω load across the entire operational bandwidth. The fabricated filter is pictured in Fig. 10(a). The performance of the fabricated filter was characterized using S-parameters ($S21_{fil}$). As seen in Fig. 11, the fabricated filter's response closely matches that of the desired antenna's response. The phase offset seen in Fig. 11(b), is due to cables which can be calibrated out.

IV. SIC MEASUREMENTS AND RF FILTER PERFORMANCE

The fabricated RF filter is shown in Fig. 10(a). Referring to Fig. 3, the signal p_{in} is first passed through the 3-dB directional coupler to obtain two identical signals each carrying half the output power. These signals are then fed to the transmit antenna and the RF-SIC filter. It should be noted that mismatch in 3-dB directional coupled and/or antenna response is

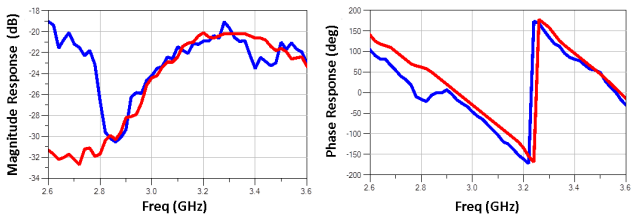

FIGURE 11. Magnitude and Phase response of the fabricated filter (shown in red) as compared to the inverted Tx/Rx antenna coupling (in blue) in Fig. 9. (a) Magnitude $S_n(j\omega)$ and, (b) Phase response $S_n(j\omega)$.

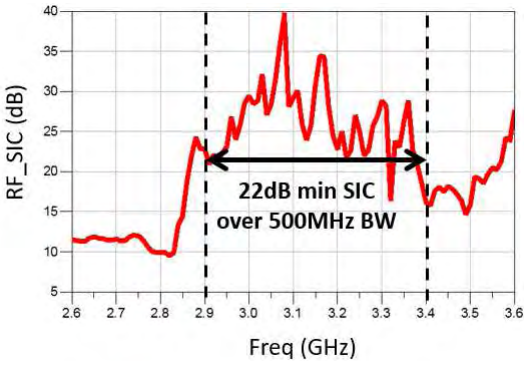

FIGURE 12. SIC achieved across the entire bandwidth.

accounted for using (9). The RF-SIC filter response serves to cancel the antenna coupled signal and therefore lowers the sensitivity of the receiver. After subtracting the filtered signal from the coupled antenna signal, the resulting RF-SIC is given by,

$$SIC_{RF}|_{(dB)} = 20log_{10}\frac{H_{fil,n}(j\omega) + H_{chnl,n}(j\omega)}{\sqrt{2}H_{chnl,n}(j\omega)}. \quad (11)$$

The derivation of SIC along with signal representation at each stage is given in detail in the Appendix. Using (9) and (26), the above can be expressed as

$$SIC_{RF}|_{(dB)} = 20log_{10}\left[\left(\frac{\Delta_{mag}{}^2(j\omega)}{2|H_{chnl,n}(j\omega)|^2}\right)+\left(1+\frac{\Delta_{mag}(j\omega)}{|H_{chnl,n}(j\omega)|}\right)\times\left(1-cos(\pm\Delta_{phase}(j\omega)\right)\right]^{\frac{1}{2}} \quad (12)$$

where $\Delta_{mag}(j\omega)$ and $\Delta_{phase}(j\omega)$ refer to the residual difference between the antenna and filter magnitude and phase response. If $H_{fil,n}(j\omega) = -H_{chnl,n}(j\omega)$ as required, then $\Delta_{mag}(j\omega) = 0$ and $\Delta_{phase}(j\omega) = 0$. For this ideal case, SIC $\rightarrow \infty$.

As seen in Fig. 11, phase and magnitude imbalances between $H_{fil,n}$ and $H_{chnl,n}$ imply a much less SIC. To calculate the RF self-interference cancellation, the transmit signal is passed through the transmit elements of the antenna array and received using a single receive element. A part of the signal is tapped to the RF-FIR filter chain using a power-divider. The coupled signal from the Rx element and the filtered signal from the RF-FIR filter chain are combined, before being fed to the LNA. At this stage, since both signals have the same magnitude but 180^0 out of phase, the signals cancel each other, providing the required cancellation. As depicted in Fig. 12, the achieved SIC is on the order of 30 dB with minimum cancellation of 22 dB. The RF-SIC is not uniform across the entire bandwidth, since the the antenna magnitude response is not uniform. Of importance is that this is achieved across very large 500 MHz bandwidth. Previous works have reported bandwidths of up to 100 MHz [2], [4], [6].

It should be noted that the target specification is to achieve a total cancellation of 100 dB across all 4 stages or an average of 50 dB between the first 2 stages. However, as mentioned before, since we are operating over unprecedented 500 MHz bandwidth, the antenna and the filter response is not uniform. Hence, the achieved RF-SIC at stage-2 is not uniform across the entire bandwidth. If the combined cancellation at the end of stage-2 is not 50 dB, the design and algorithm at stage-3 and 4 are adjusted accordingly to provide better isolation at those frequencies.

V. CONCLUSION

We proposed a wideband multi-stage self-interference cancellation STAR system. Previous designs have been limited to bandwidths less than 100 MHz, whereas the proposed STAR system achieved 500 MHz. Our design employed a higher order FIR filter with added degrees of freedom to achieve large cancellation bandwidths. Specifically, both amplitude weights and time delays were considered as adjustable variables at each of the filter taps. Also, for the first time, our cancellation process accounted for coupling effects among the surrounding antenna elements within the array. Measurements showed a cancellation level of 22 dB to 40 dB across 500 MHz using a 6^{th} order RF-SIC filter. To our knowledge, this is the most wideband self-interference cancellation. Future work will involve novel filter design to achieve consistent cancellation of 30 dB or more over wider bandwidth.

Appendix

From Fig. 3, the signal at the input of the LNA in the receiver chain from a single transmit element is given by,

$$r_{RF} = r_{fil}S13_{RxC} + r_{chnl}S12_{RxC} \quad (13)$$

where

$$r_{fil} = p_{in}S31_{TxC}S21_{fil}$$
$$r_{chnl} = p_{in}S21_{TxC}S21_{chnl}. \quad (14)$$

Thus (13) can be represented as,

$$r_{RF} = p_{in}\underbrace{S31_{TxC}S21_{fil}S13_{RxC}}_{T_1} + p_{in}\underbrace{S21_{TxC}S21_{chnl}S12_{RxC}}_{T_2} \quad (15)$$

where

$$T_1 = |S31_{TxC}||S21_{fil}||S13_{RxC}| \angle(S31_{TxC} + S21_{fil} + S13_{RxC})$$
$$T_2 = |S21_{TxC}||S21_{chnl}||S12_{RxC}| \angle(S21_{TxC} + S21_{chnl} + S12_{RxC}). \quad (16)$$

That is, (13) can be expressed as

$$r_{RF} = p_{in} r'_{RF} \quad (17)$$

where $r'_{RF} = T_1 + T_2$.

Therefore, $|r'_{RF}|^2$ can be expressed as

$$|r'_{RF}|^2 = |T_1 + T_2|^2 = |T_1|^2 + |T_2|^2 + 2|T_1||T_2|cos(\angle T_1 - \angle T_2) \quad (18)$$

implying

$$|r'_{RF}|^2 = \underbrace{|S31_{TxC}|^2|S21_{fil}|^2|S13_{RxC}|^2}_{|T_1|^2} + \underbrace{|S21_{TxC}|^2|S21_{chnl}|^2|S12_{RxC}|^2}_{|T_2|^2} + \Bigg(\underbrace{2|S31_{TxC}||S21_{fil}||S13_{RxC}|}_{2|T_1|} \times \underbrace{|S21_{TxC}||S21_{chnl}||S12_{RxC}|}_{|T_2|} \times cos\Big(\underbrace{\angle(S31_{TxC} + S21_{fil} + S13_{RxC})}_{\angle T_1} - \underbrace{\angle(S21_{TxC} + S21_{chnl} + S12_{RxC})}_{\angle T_2} \Big) \Bigg). \quad (19)$$

Using the condition specifed in (7) the above expression becomes,

$$|r'_{RF}|^2 = \frac{|S21_{fil}|^2}{4} + \frac{|S21_{chnl}|^2}{4} + \frac{2|S21_{fil}||S21_{chnl}|}{4} cos\big(\angle S21_{fil} - \angle S21_{chnl}\big). \quad (20)$$

In the above equation (20) it was assumed that there is no phase imbalance between the transmit and receive direction couplers. That is,

$$\angle S31_{TxC} = \angle S21_{TxC}$$
$$\angle S13_{RxC} = \angle S12_{RxC}. \quad (21)$$

Following a similar analysis as above, the coupled signal from the antenna is given by,

$$r_{chnl} = p_{in} S21_{TxC} S21_{chnl} = p_{in} r'_{chnl} \quad (22)$$

with

$$|r'_{chnl}|^2 = |S21_{TxC}|^2|S21_{chnl}|^2 = \frac{|S21_{chnl}|^2}{2}. \quad (23)$$

The, RF-SIC is then given by

$$SIC_{RF}|_{(dB)} = 20log_{10}\frac{r_{RF}}{r_{chnl}}. \quad (24)$$

Using (14), (20) and (23), the above equation reduces to,

$$SIC_{RF}|_{(dB)} = 20log_{10}\Bigg[\frac{1}{2|S21_{chnl}|^2}\Big(|S21_{fil}|^2 + |S21_{chnl}|^2 + 2|S21_{fil}||S21_{chnl}|cos\big(\angle S21_{fil} - \angle S21_{chnl}\big)\Big)\Bigg]^{\frac{1}{2}}. \quad (25)$$

Using (4) and (5), the above expression can be re-written as

$$SIC_{RF}|_{(dB)} = 20log_{10}\Bigg[\frac{1}{2|H_{chnl,n}|^2}\Big(|H_{fil,n}|^2 + |H_{chnl,n}|^2 + 2|H_{fil,n}||H_{chnl,n}|cos\big(\angle H_{fil,n} - \angle H_{chnl,n}\big)\Big)\Bigg]^{\frac{1}{2}}. \quad (26)$$

REFERENCES

[1] S. Hong *et al.*, "Applications of self-interference cancellation in 5G and beyond," *IEEE Commun. Mag.*, vol. 52, no. 2, pp. 114–121, Feb. 2014.

[2] K. E. Kolodziej, J. G. McMichael, and B. T. Perry, "Multitap RF canceller for in-band full-duplex wireless communications," *IEEE Trans. Wireless Commun.*, vol. 15, no. 6, pp. 4321–4334, Jun. 2016.

[3] L. Larson, "RF and microwave hardware challenges for future radio spectrum access," *Proc. IEEE*, vol. 102, no. 3, pp. 321–333, Mar. 2014.

[4] J. Zhou, T.-H. Chuang, T. Dinc, and H. Krishnaswamy, "Integrated wideband self-interference cancellation in the RF domain for FDD and full-duplex wireless," *IEEE J. Solid-State Circuits*, vol. 50, no. 12, pp. 3015–3031, Dec. 2015.

[5] M. Duarte and A. Sabharwal, "Full-duplex wireless communications using off-the-shelf radios: Feasibility and first results," in *Proc. Conf. Rec. 44th Asilomar Conf. Signals, Syst. Comput.*, Nov. 2010, pp. 1558–1562.

[6] D. Bharadia and S. Katti, "Full duplex MIMO radios," in *Proc. 11th USENIX Conf. Netw. Syst. Design Implement.*, 2014, pp. 359–372.

[7] D.-J. van den Broek, E. A. M. Klumperink, and B. Nauta, "A self-interference-cancelling receiver for in-band full-duplex wireless with low distortion under cancellation of strong TX leakage," in *IEEE Int. Solid-State Circuits Conf. (ISSCC) Dig. Tech. Papers*, Feb. 2015, pp. 1–3.

[8] H. Holma, S. Heikkinen, O. A. Lehtinen, and A. Toskala, "Interference considerations for the time division duplex mode of the UMTS terrestrial radio access," *IEEE J. Sel. Areas Commun.*, vol. 18, no. 8, pp. 1386–1393, Aug. 2000.

[9] H. Haas and G. J. R. Povey, "The effect of adjacent channel interference on capacity in a hybrid TDMA/CDMA-TDD system using UTRA-TDD parameters," in *Proc. IEEE VTS 50th Veh. Technol. Conf. (VTC-Fall)*, vol. 2. Sep. 1999, pp. 1086–1090.

[10] S. Chen, M. A. Beach, and J. P. McGeehan, "Division-free duplex for wireless applications," *Electron. Lett.*, vol. 34, no. 2, pp. 147–148, Jan. 1998.

[11] D. Bharadia, E. McMilin, and S. Katti, "Full duplex radios," in *Proc. Conf. SIGCOMM ACM*, New York, NY, USA, 2013, pp. 375–386.

[12] K. L. Scherer *et al.*, "Simultaneous transmit and receive system architecture with four stages of cancellation," in *Proc. IEEE Int. Symp. Antennas Propag. USNC/URSI Nat. Radio Sci. Meeting*, Jul. 2015, pp. 520–521.

[13] S. Bojja-Venkatakrishnan, E. A. Alwan, and J. L. Volakis, "Wideband RF and analog self-interference cancellation filter for simultaneous transmit and receive system," in *Proc. IEEE Int. Symp. Antennas Propag. USNC/URSI Nat. Radio Sci. Meeting*, Jul. 2017, pp. 933–934.

[14] S. J. Watt, E. A. Alwan, W. Khalil, and J. L. Volakis, "Wideband self-interference cancellation filter for simultaneous transmit and receive systems," in *Proc. IEEE Int. Symp. Antennas Propag. USNC/URSI Nat. Radio Sci. Meeting*, Jul. 2015, pp. 129–130.

[15] T. Dinc and H. Krishnaswamy, "A T/R antenna pair with polarization-based reconfigurable wideband self-interference cancellation for simultaneous transmit and receive," in *Proc. IEEE MTT-S Int. Microw. Symp.*, May 2015, pp. 1–4.
[16] E. Yetisir, C.-C. Chen, and J. L. Volakis, "Low-profile UWB 2-port antenna with high isolation," *IEEE Antennas Wireless Propag. Lett.*, vol. 13, pp. 55–58, 2014.
[17] A. Goel, B. Analui, and H. Hashemi, "Tunable duplexer with passive feed-forward cancellation to improve the RX-TX isolation," *IEEE Trans. Circuits Syst. I, Reg. Papers*, vol. 62, no. 2, pp. 536–544, Feb. 2015.
[18] A. Sabharwal, P. Schniter, D. Guo, D. W. Bliss, S. Rangarajan, and R. Wichman, "In-band full-duplex wireless: Challenges and opportunities," *IEEE J. Sel. Areas Commun.*, vol. 32, no. 9, pp. 1637–1652, Sep. 2014.
[19] J. Zhou, P. R. Kinget, and H. Krishnaswamy, "A blocker-resilient wideband receiver with low-noise active two-point cancellation of >0 dBm TX leakage and TX noise in RX band for FDD/Co-existence," in *IEEE Int. Solid-State Circuits Conf. (ISSCC) Dig. Tech. Papers*, Feb. 2014, pp. 352–353.
[20] M. Duarte, C. Dick, and A. Sabharwal, "Experiment-driven characterization of full-duplex wireless systems," *IEEE Trans. Wireless Commun.*, vol. 11, no. 12, pp. 4296–4307, Dec. 2012.
[21] J. I. Choi, M. Jain, K. Srinivasan, P. Levis, and S. Katti, "Achieving single channel, full duplex wireless communication," in *Proc. 16th Annu. Int. Conf. Mobile Comput. Netw.*, 2010, pp. 1–12.
[22] M. Jain *et al.*, "Practical, real-time, full duplex wireless," in *Proc. 17th Annu. Int. Conf. Mobile Comput. Netw.*, 2011, pp. 301–312.
[23] E. Everett, A. Sahai, and A. Sabharwal, "Passive self-interference suppression for full-duplex infrastructure nodes," *IEEE Trans. Wireless Commun.*, vol. 13, no. 2, pp. 680–694, Jan. 2014.
[24] B. Debaillie *et al.*, "Analog/RF solutions enabling compact full-duplex radios," *IEEE J. Sel. Areas Commun.*, vol. 32, no. 9, pp. 1662–1673, Sep. 2014.
[25] J. Choma, "Scattering parameters: Concept, theory, and applications," Univ. Southern California, Los Angeles, CA, USA, Tech. Rep. EE 541, # 2, 2006.
[26] D. K. Papantonis and J. L. Volakis, "Dual-polarized tightly coupled array with substrate loading," *IEEE Antennas Wireless Propag. Lett.*, vol. 15, pp. 325–328, 2016.
[27] I. J. Gupta and A. A. Ksienski, "Effect of mutual coupling on the performance of adaptive arrays," *IEEE Trans. Antennas Propag.*, vol. 31, no. 5, pp. 785–791, Sep. 1983.
[28] R. Janaswamy, "Effect of element mutual coupling on the capacity of fixed length linear arrays," *IEEE Antennas Wireless Propag. Lett.*, vol. 1, pp. 157–160, 2002.

SATHEESH BOJJA VENKATAKRISHNAN was born in Tiruchirappalli, India, in 1987. He received the bachelor's degree in electronics and communication engineering from the National Institute of Technology, Tiruchirappalli, in 2009, and the M.S. and Ph.D. degrees in electrical engineering from The Ohio State University, Columbus, OH, USA, in 2017. He was a Scientist with DRDO, India, from 2009 to 2013, involved in the development and implementation of active electronic steerable antennas, with main focus on beam forming. He has been a Post-Doctoral Associate with the Florida International University, since 2017. His current research includes receiver design for communication circuits, RF systems, and digital signal processing using FPGAs. He is also involved in simultaneous transmit and receive system, to improve the spectral efficiency. He has been a Phi Kappa Phi member, since 2015. He received the second prize in International Union of Radio Science General Assembly and Scientific Symposium student paper competition held at Montreal, Canada, in 2017. He was a recipient of the Student Paper Competition Honorable Mention at the IEEE Antenna and Propagation Symposium in 2015 and 2016, and the Student Fellowship Travel Grant Award from the U.S. National Committee for the International Union of Radio Science in 2016 and 2017.

ELIAS A. ALWAN (GS'07–M'10) was born in Aitou, Lebanon, in 1984. He received the B.E. degree *(summa cum laude)* in computer and communication engineering from Notre Dame University–Louaize, Zouk Mosbeh, Lebanon, in 2007, the M.E. degree in electrical engineering from the American University of Beirut, Beirut, Lebanon, in 2009, and the Ph.D. degree in electrical and computer engineering from The Ohio State University (OSU), Columbus, OH, USA, in 2014. He was a Senior Research Associate with the ElectroScience Laboratory, OSU from 2015 to 2017. He is currently an Assistant Professor with the ECE Department, Florida International University. His research is in the areas of antennas and radio frequency systems with particular focus on ultra-wideband (UWB) communication systems, including UWB arrays, reduced hardware and power efficient communication back-ends, and millimeter-wave technologies for 5G applications. He has been a Phi Kappa Phi member since 2010.

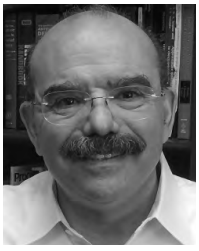

JOHN L. VOLAKIS (S'77–M'82–SM'89–F'96) was born in Chios, Greece, in 1956 and immigrated to the USA. in 1973. He received the B.E. degree *(summa cum laude)* from Youngstown State University, Youngstown, OH, USA, in 1978, and the M.Sc. and Ph.D. degrees from The Ohio State University, Columbus, in 1979 and 1982, respectively. He was with Boeing Phantom Works from 1982 to 1984. In 1984, he was an Assistant Professor with the University of Michigan, Ann Arbor, and become a Full Professor in 1994. He also served as the Director of the Radiation Laboratory from 1998 to 2000. From 2003 to 2017, he served as the Roy and Lois Chope Chair Professor of Engineering with The Ohio State University, and also as the Director of the ElectroScience Laboratory. Since 2017, he has been the Dean of Engineering with the Florida International University. He has authored or co-authored over 280 articles in major refereed journals, nearly 500 conference papers and 20 book chapters. He co-authored the following six books: *Approximate Boundary Conditions in Electromagnetics* (Institution of Electrical Engineers, London, 1995), *Finite Element Method for Electromagnetics* (IEEE Press, New York, 1998), *Frequency Domain Hybrid Finite Element Methods in Electromagnetics* (Morgan & Claypool, 2006), *Computational Methods for High Frequency Electromagnetic Interference* (Verlag, 2009), *Small Antennas* (McGraw-Hill, 2010), and edited the *Antenna Engineering Handbook* (McGraw-Hill, 2007). He has also written several well-edited coursepacks on introductory and advanced numerical methods for electromagnetics, and has delivered short courses on antennas, numerical methods, and frequency selective surfaces. His primary research deals with antennas, computational methods, electromagnetic compatibility and interference, propagation, design optimization, RF materials, multi-physics engineering, and bioelectromagnetics. He is a member of the URSI Commissions B and E. He received the University of Michigan (UM) College of Engineering Research Excellence Award in 1998, the UM, Department of Electrical Engineering and Computer Science Service Excellence Award in 2001, and The Ohio State Univ. Clara and Peter Scott Award for outstanding academic achievement in 2010. He is listed by ISI among the top 250 most referenced authors. He graduated/mentored about 85 Ph.D. students/post-docs, and co-authored with them for 14 Best Paper Awards at conferences. He was the President of the IEEE Antennas and Propagation Society in 2004 and served on the AdCom of the IEEE Antennas and Propagation Society from 1995 to 1998. He also served as an Associate Editor for the IEEE Transactions on Antennas and Propagation from 1988 to1992, Radio Science from 1994 to1997, and for the *IEEE Antennas and Propagation Society Magazine* from 1992 to2006, the *Journal of Electromagnetic Waves and Applications* and the URSI Bulletin. He was a Chair of the IEEE Antennas and Propagation Society Symposium and Radio Science Meeting in Ann Arbor, MI, USA, in 1993 and a Co-Chair of the same Symposium in Columbus, OH, USA, in 2003.